MonoPHY: Mono-Stream-based Device-free WLAN Localization via Physical Layer Information

Heba Abdel-Nasser, Reham Samir, Ibrahim Sabek
Comp. Sys. and Eng. Department
Alexandria University, Egypt
{heba.naser, reham.abouras, ibrahim.sabek}@alexu.edu.eg

Moustafa Youssef
Wireless Research Center
Alexandria University and E-JUST, Egypt
moustafa.youssef@ejust.edu.eg

***Abstract*—Device-free (DF) indoor localization has grasped great attention recently as a value-added service to the already installed WiFi infrastructure as it allows the tracking of entities that do not carry any devices nor participate actively in the localization process. Current approaches, however, require a relatively large number of wireless streams, i.e. transmitter-receiver pairs, which is not available in many typical scenarios, such as home monitoring.**

In this paper, we introduce *MonoPHY* as an accurate mono-stream device-free WLAN localization system. *MonoPHY* leverages the physical layer information of WiFi networks supported by the IEEE 802.11n standard to provide accurate DF localization with only one stream. In particular, *MonoPHY* leverages both the low-level *Channel State Information* and the MIMO information to capture the human effect on signal strength. Experimental evaluation in a typical apartment, with a side-by-side comparison with the state-of-the-art, shows that *MonoPHY* can achieve an accuracy of $1.36m$. This corresponds to at least 48% enhancement in median distance error over the state-of-the-art DF localization systems using a single stream only.

***Index Terms*—Device-free localization, detection and tracking, physical-layer based localization.**

I. Introduction

Many localization systems have been proposed over the years including the GPS systems [1], RF-based systems [2]–[6], inertial-based systems [7]–[9], and infrared-based systems [10]. All these systems require that the tracked entity carries a device. On the other hand, device-free passive (DfP) localization [11] is based on using typical wireless networks to detect and track entities that do not carry any devices nor participate actively in the localization process. It depends on the fact that the RF signal strength is affected by human motion. DfP localization can be used in many applications including smart homes, intrusion detection, and traffic estimation. A typical DfP system consists of signal transmitters (such as standard access points (APs)), monitoring points (MPs) (such as standard laptops or APs themselves), and an application server for processing.

Current approaches for DfP localization include radar-based systems, e.g. [12]–[14], computer vision based systems, e.g. [15], [16] and Radio Tomographic Imaging (RTI), e.g. [17]. These systems, however, need special hardware and high installation cost. On the contrary, a number of DfP localization systems have been proposed that operate in standard WiFi networks, e.g. [18]–[28], without requiring any additional equipment. Therefore, these systems provide a value added-service on top of the wireless infrastructure, just based on the reported signal strength from the MAC layer. Nevertheless, they still require a large number of streams (a data stream is the data received from one AP at one MP), which limits their applicability and accuracy in a large class of scenarios, such as in homes, where usually a small number, typically one AP is installed.

In this paper, we introduce *MonoPHY* as a ***single*** stream DF localization system. To compensate for the reduced number of streams, *MonoPHY* leverages the available detailed **physical layer** information of WiFi networks. In particular, the IEEE 802.11n standard uses the OFDM modulation, where a wide channel is divided into several orthogonal subcarriers each arriving at the location of the receiver with distinct values of phase and magnitude (denoted as Channel State Information (CSI)). This provides rich information to detect the effect of human motion on the magnitude of each subcarrier, as compared to a single signal strength value that has been used with the current approaches. In addition, the IEEE 802.11n devices use the MIMO technology, which further provides more information about each antenna pair from the transmitter to the receiver.

MonoPHY captures the effect of the human standing at different locations in the area of interest on the CSI vectors that describe the channel performance at each OFDM subcarrier on each MIMO antenna pair at the receiver in a training phase. This CSI data at each location is modeled as Gaussian mixtures and stored in what we call an RF fingerprint. During the operation phase, few samples are collected at each MP, which are further compared with each entry in the fingerprint map to determine the closest location.

Experimental evaluation, in a typical apartment using a single access point and a single laptop with an Intel 5300 wireless card shows that *MonoPHY* can achieve a localization accuracy of less than 1.36m using a ***single*** stream. This corresponds to at least 48.1% enhancement in median error over the state-of-the-art DF localization systems using the same WLAN installation.

The rest of the paper is organized as follows: Section II presents a brief background about the physical layer information used in *MonoPHY* and its properties that can be used to identify the human location based. Section III discusses

978-1-4673-5939-9/13/$31.00 ©2013 IEEE

the system architecture and the proposed model. We evaluate *MonoPHY* in a typical WiFi testbed and compare it to the state-of-the-art DF WLAN localization techniques in Section IV. Finally, we conclude the paper and give directions for future work in Section V.

II. Background and CSI Characterization

In this section, we introduce the necessary background on the physical layer information we use along with the basic principles our system is based on.

A. Channel State Information (CSI)

Most WLANs, including IEEE 802.11a/g/n, use OFDM modulation in which signals are transmitted over several orthogonal frequencies called subcarriers. The OFDM channel is a wide channel divided into subcarriers where each signal, transmitted on a subcarrier, has a different signal strength and phase. Typical wireless cards provide received signal strength information as received from the MAC layer, which represents a fused value that captures the wireless channel between the transmitter and receiver, **regardless of the number of antennas or subcarriers** between them.

On the other hand, some of the common IEEE 802.11n standard based cards available in the market, e.g. the Intel 5300 card, provides detailed information about the physical layer of the RF channel represented as *Channel State Information* (CSI), which provides the signal strength and phase of the OFDM subcarriers between each pair of transmitter and receiver antennas. In particular, the Intel 5300 card reports the CSI for 30 groups of subcarriers, which is about one group for every 2 subcarriers for the 20MHz channels operating on the 2.4GHz frequency [29].

B. MIMO Technology

The IEEE 802.11n nodes also use another technology which is Multiple-Input Multiple-Output (MIMO). In MIMO, there are multiple transmitter and receiver antennas, where each combination of receiver and transmitter antennas can be considered as a separate stream. This facility provides multiple virtual streams between a transmitter-receiver pair and hence should lead to better accuracy.

C. CSI Properties

In this section, we show some of the properties of CSI that can be used to identify the human location based on changes of the CSI. Due to space constraints, we focus on the CSI magnitude in this paper and leave leveraging phase information to a future paper.

Figure 1(a) shows the probability density function (pdf) for the CSI magnitude for a single virtual stream (signal strength of one subcarrier of one link). The figure shows that this pdf fits a Gaussian distribution mixture nicely, which confirms to previous analysis [30].

Figures 1(b) and 1(c) show the CSI magnitude for one stream over different packets (each packet is represented by a line) for the 30 subcarriers. We can notice from the figure that the CSI values for each stream form clusters. In Figure 1(b), two clusters are formed while in Figure 1(c) the CSI values form only one cluster. Although the number of clusters for each location in the fingerprint map is variable, we found that it does not exceed three clusters. This observation simplifies the clustering operation and allows the usage of efficient techniques in terms of running time (e.g. k-means algorithm).

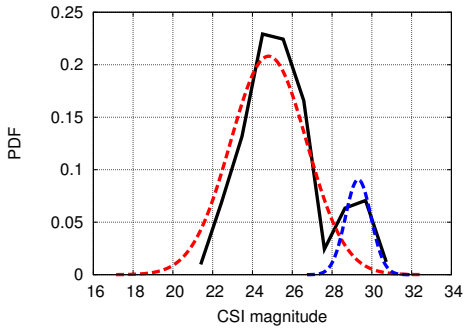

(a) PDF of the CSI magnitude showing the Gaussian mixture representing the two clusters.

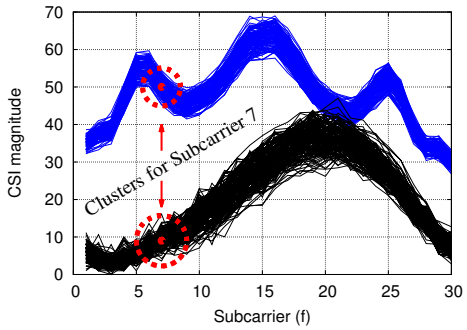

(b) Link with two clusters. For a specific subcarrier, the signal strength magnitude samples over different received packets have two clusters (blue and black), each can be modeled by a Gaussian distribution (as in Subfigure a).

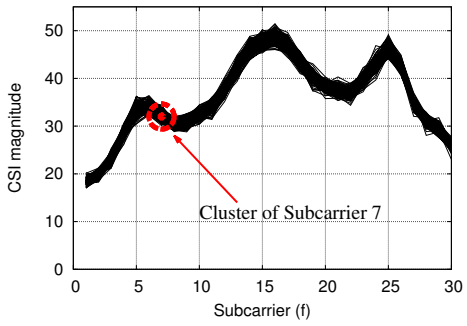

(c) Link with one cluster. For a specific subcarrier, the signal strength magnitude samples over different received packets can be modeled by a Gaussian distribution.

Fig. 1: Channel State Information properties for one link (one transmitter-receiver antennas pair). Each line represents the CSI magnitude of one packet over all subcarriers. Different lines represent different packets.

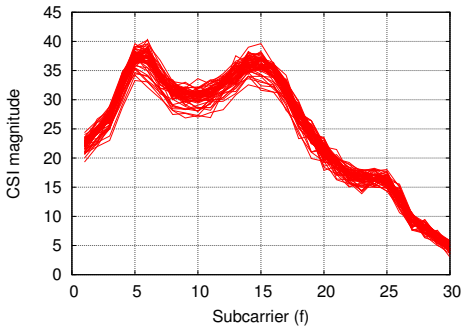

(a) Silence (no human)

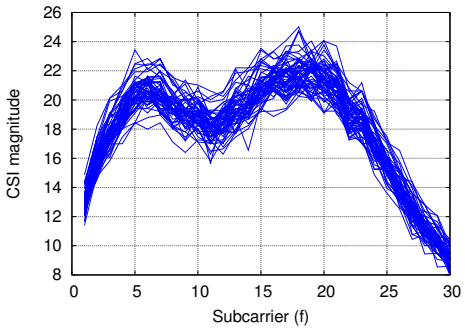

(b) Human at Location 1

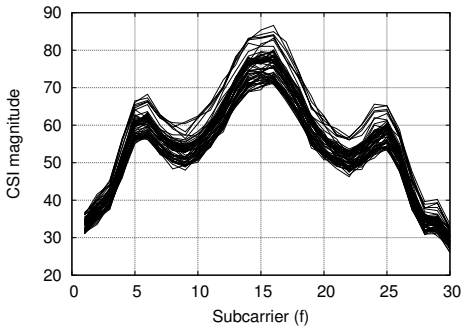

(c) Human at Location 2

Fig. 2: Channel State Information magnitudes for different human presence/location scenarios.

Figure 2 shows the CSI magnitude for the silence case as well as the presence of the human at two different locations for one stream. The figure shows that the CSI magnitude information can be used to identify the human presence as well as determine her location.

III. The MonoPHY System

In this section, we give the details of *MonoPHY*. We start by an overview of the system architecture, the system model, and the system details.

A. Overview

Figure 3 shows the system architecture. We have two phases of operation, offline and online phases:

The **Offline training phase** is used to build a clusters-based fingerprint. During this phase, a person stands at different

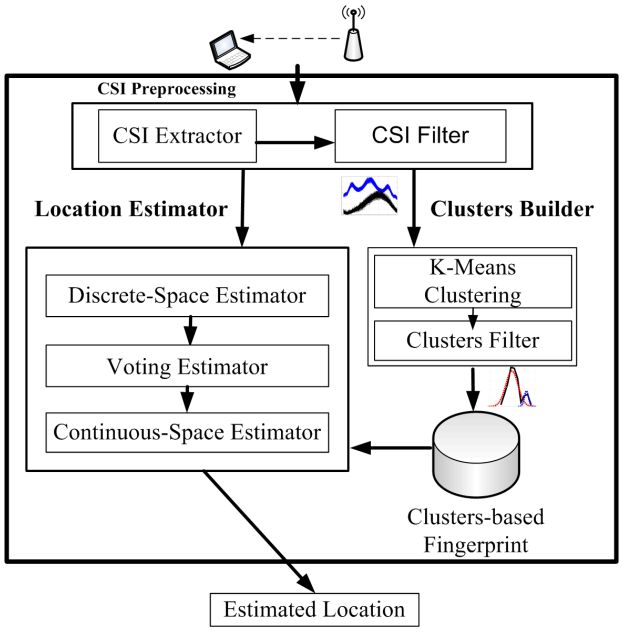

Fig. 3: System Architecture

locations in the area of interest. For each location, CSI values are recorded for all transmitter-receiver pairs and used to construct clusters to discriminate this location from others.

The **Online localization phase** is used to estimate the entity location based on the currently collected CSI for each transmitter-receiver pair and the clusters-based fingerprint prepared in the offline phase.

The *CSI Preprocessing* module extracts CSI values from sent packets for each stream and filters outlier values.

The *Clusters Builder* module constructs discriminative clusters for locations using the k-means algorithm. Each subcarrier at every fingerprint location is represented by up to three clusters as discussed in Section II-C. Clusters with members below a threshold are filtered out.

The *Location Estimator* module calculates the minimum distance between the currently collected CSI in the online phase and the stored clusters, selects a set of candidate locations, and estimates the most probable location. It has two modules: one for the discrete-space estimation and the other for the continuous-space estimation.

B. System Model

Assume a DF system installed in an area with l fingerprint locations. This area is covered by only one AP (with n MIMO antennas) and one MP (laptop with a card with m MIMO antennas). This leads to $n.m$ *virtual links* between the transmitter and receiver. Using the OFDM modulation, each transmitted packet is sent using f subcarriers on each of the n antennas. This leads to a total of $n.m.f$ *virtual signal strength streams* at the receiver, where each stream corresponds to one carrier for each virtual link.

Based on the discussion in Section II-C, the signal strength of each virtual stream can be mapped into k clusters, $k \leq 3$,

where each cluster is represented by a mixture of up to k Gaussian random variables (see e.g. Figure 1a). Let $\mathbb{R}$ represents the entire fingerprint. Therefore, the fingerprint at each radio map location (R_l) can be represented by a vector $R_l = (U, V)$, where $U = U_{i,j}^{a,b}$ and $V = V_{i,j}^{a,b}$ represent the mean and variance (respectively) of the Gaussian random variable representing the signal strength received from transmitter antenna i at receiver antenna j on subcarrier a of cluster b.

Therefore, the problem becomes, given a received packet with an associated signal strength vector $S = (s_{1,1}^1, s_{1,1}^2, \cdots, s_{n,m}^f)$, where $s_{i,j}^a$ represents the CSI magnitude of the packet received from transmitter antenna i at receiver antenna j on subcarrier a, we want to estimate the most probable entity location. In the next subsection, we assume a discrete space while in Section III-D we handle the continuous space case[1].

C. MonoPHY Discrete-Space Estimator

Given the received signal strength vector S, we want to find the location l^* in the fingerprint that maximizes the probability $P(l|S)$. That is:

$$l^* = \arg\max_l P(l|S) \tag{1}$$

Using Baysian inversion, this can be represented as:

$$l^* = \arg\max_l \frac{P(S|l).P(l)}{P(S)} \tag{2}$$

Assuming all locations are equally likely[2] and noting that $P(S)$ is independent of l, Equation 2 becomes:

$$l^* = \arg\max_l P(S|l) \tag{3}$$

$P(S|l)$ can be estimated from the constructed fingerprint, $\mathbb{R}$, as

$$P(S|l) = \max_b \prod_{a=1}^{f} \prod_{i=1}^{n} \prod_{j=1}^{m} \int_{s_{i,j}^f - \frac{1}{2}}^{s_{i,j}^f + \frac{1}{2}} \frac{1}{2\pi (V_{ij}^{a,b})^2} \exp\left(- \frac{(x - U_{ij}^{a,b})^2}{2 (V_{ij}^{a,b})^2} \right) \mathrm{d}x \tag{4}$$

where $U_{i,j}^{a,b}$ and $V_{ij}^{a,b}$ are the mean and variance vectors of the Gaussian mixtures as defined in the system model and the constant $\frac{1}{2}$ represents the quantization interval of signal strength.

To improve the robustness of the localization output, we apply Equation 4 on a sequence of packets during a time window w. A voting process is applied on all location candidates obtained during the window, where the fingerprint location with the highest vote is returned as the most probable location.

[1]Note that the silence case (i.e. when no entity is present in the area of interest) can be treated as a special location with its own fingerprint.

[2]If the probabilities distribution of $P(l)$ is known, it can be used directly in Equation 2

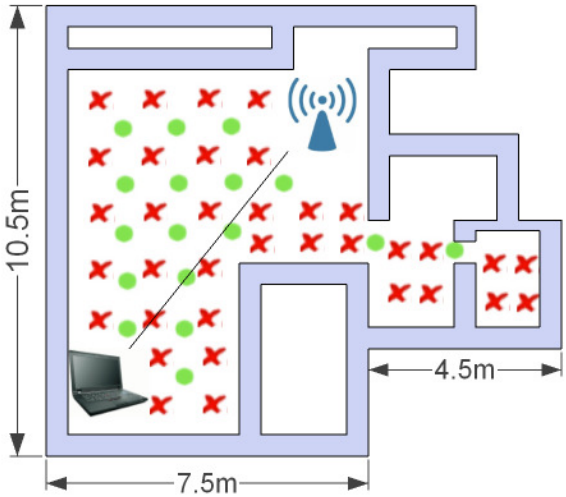

Fig. 4: Experimental testbed with training locations (red crosses) and testing locations (green circles)

D. MonoPHY Continuous-Space Estimator

The previous estimator will always return one of the fingerprint locations, even if the entity is standing in between. To further enhance accuracy, the continuous space estimator estimates the location as the weighted average of the most probable r locations, where each location is weighed by its probability normalized by the sum over all probabilities.

IV. Performance Evaluation

In this section, we analyze the performance of *MonoPHY* and compare it to the state-of-the-art DF WLAN localization systems [20], [31]. We start by describing the experimental setup and data collection. Then, we analyze the effect of different parameters on the system performance. We end the section by a comparison with the state-of-the-art.

A. Testbed and Data Collection

We evaluated *MonoPHY* in a typical apartment with an area of approximately $100m^2$ (about 1077 sq. ft.) as shown in Figure 4. The area was covered by a single Cisco Linksys X2000 AP and a Dell Adamo XPS laptop as a MP. The laptop has an Intel 5300 card that can provide CSI information [29]. The fingerprint is constructed for 35 different locations, uniformly distributed over the testbed area. An independent test set of 17 locations are chosen randomly between the training locations at different times of day using different persons from the training set.

Table I shows the default values for the different parameters.

B. Effect of Different Parameters

1) Effect of the number of receiver antennas (m): Figure 5 shows the effect of changing the antennas combinations on the median distance error. The figure shows that different combinations lead to different accuracy. This is due to the noisy wireless channel and the different multipath effects

Parameter	Default value	Meaning
m	2	Num. of receiver antennas
n	1	Num. of transmitter antennas
r	6	Num. of averaged locations
w	20	Window size for votes
f	20	Num. of subcarriers

TABLE I: Default parameters values.

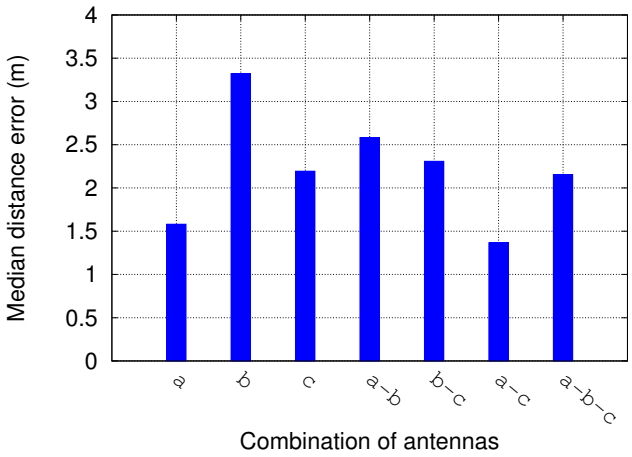

Fig. 5: Effect of different combinations of receiver antennas (a, b, c).

encountered by the packets received at the different antennas. This means that using more antennas does not necessarily lead to better accuracy. The good news is that the SNR associated with the antennas can be used to determine the best combination. For the rest of this section, we use antennas a and c (i.e. $m = 2$) as they lead to the best accuracy.

2) Effect of the time window size for voting (w): Figure 6 shows the effect of increasing w. The figure shows that as the window size used for voting increases, the accuracy increases. However, increasing w increases the latency. Therefore, there is a tradeoff that a designer needs to balance based on her needs. Using $w = 20$ gives high accuracy of $1.36m$ with reasonable latency.

3) Effect of processed subcarriers (f): Figure 7 shows the effect of increasing the number of subcarriers on the median distance error. The figure shows that increasing the number of subcarriers leads to better accuracy until it saturates at about 20 subcarriers.

4) Effect of number of averaged locations (r): Figure 8 shows the effect of increasing the number of averaged locations (r) for the continuous-space estimator. The figure shows that increasing the number of averaged locations reduces the median distance error until it saturates around $r = 6$.

C. Comparison with the State-of-the-Art

Figure 9 shows the CDF of the distance error for the discrete-space and continuous-space estimators of *MonoPhy* as compared to the Deterministic [20] and Probabilistic Nuzzer [31] traditional DF systems. Table II summarizes the results. The results show that *MonoPhy* has the best accuracy with

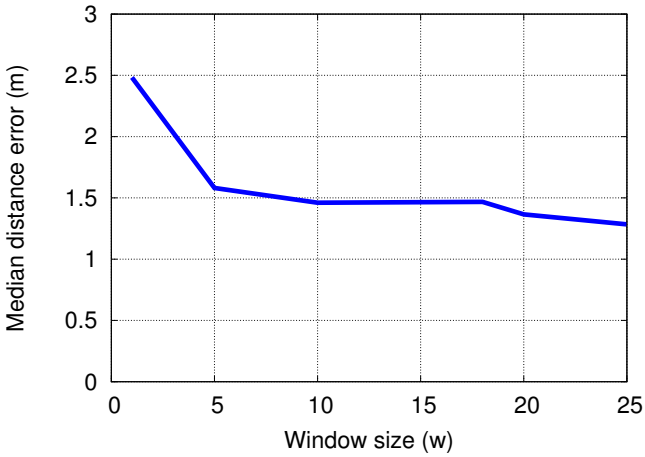

Fig. 6: Effect of the time window size used for voting (w).

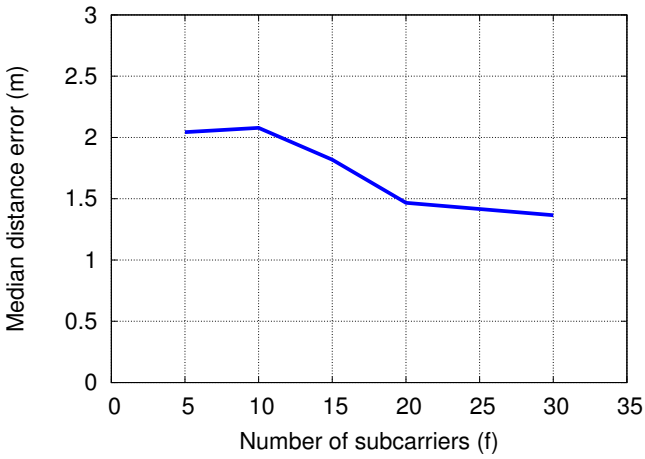

Fig. 7: Effect of the number of subcarriers used.

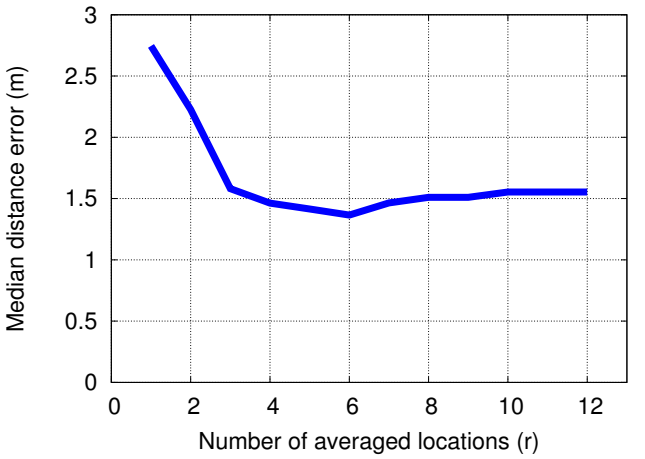

Fig. 8: Effect of the number of averaged locations (r).

an enhancement of at least 48.1% in median distance error over the best state-of-the-art techniques **using only a single stream**.

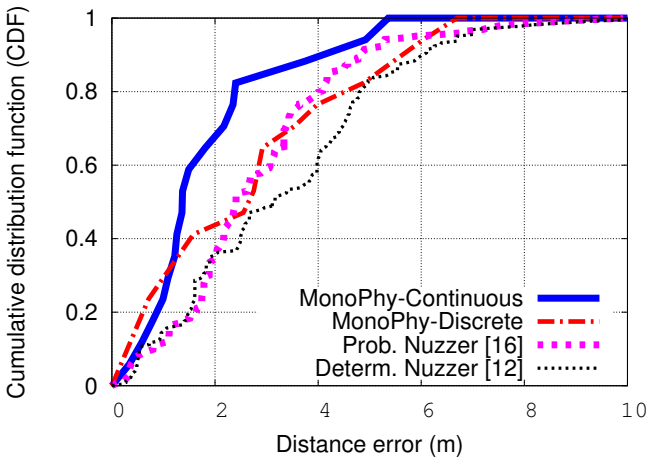

Fig. 9: CDF of distance error for the different systems.

Technique	Median distance error	Percentage enhancement of *MonoPHY-Cont*
Determ. Nuzzer	3.16	56.81%
Prob. Nuzzer	2.63	48.10%
MonoPHY-Discrete	2.75	50.34%
MonoPHY-Cont	1.36	N/A

TABLE II: Comparison between MonoPHY and the state-of-the-art techniques.

V. Conclusion

We presented the design, analysis, and implementation of *MonoPHY*: an accurate device-free WLAN localization system based on a single stream. *MonoPHY* leverages *Channel State Information* (CSI) from the physical layer as well as the MIMO information to achieve its high accuracy with limited hardware.

Experimental evaluation in a typical WiFi testbed shows that *MonoPHY* can achieve $1.36m$ median distance error, which is better than the state-of-the-art techniques by at least 48%. This highlights the promise of *MonoPHY* for real-time DF tracking applications.

Currently, we are expanding *MonoPhy* in multiple directions including integrating the CSI phase information, multiple entities detection and tracking, and entity identification.

Acknowledgment

This work is supported in part by a grant from the Egyptian Science and Technology Development Fund (STDF).

References

[1] P. Enge and P. Misra, "Special Issue on Global Positioning System," in *Proceedings of the IEEE, January 1999*, 1999, pp. 3–172.

[2] M. A. Youssef and A. Agrawala, "The Horus WLAN Location Determination System," in *ACM MobiSys*, 2005, pp. 205–218.

[3] M. Ibrahim and M. Youssef, "CellSense: An accurate energy-efficient GSM positioning system," *IEEE T. Vehicular Technology*, vol. 61, no. 1, pp. 286–296, 2012.

[4] ——, "A hidden Markov model for localization using low-end GSM cell phones," in *ICC*, 2011, pp. 1–5.

[5] M. Youssef and M. Abdallah, "Multivariate analysis for probabilistic WLAN location determination systems," in *MobiQuitous*, 2005, pp. 353–362.

[6] M. Ibrahim and M. Youssef, "Cellsense: A probabilistic RSSI-based GSM positioning system," in *GLOBECOM*, 2010, pp. 1–5.

[7] M. Youssef, M. A. Yosef, and M. N. El-Derini, "GAC: Energy-efficient hybrid GPS-accelerometer-compass GSM localization," in *GLOBECOM*, 2010, pp. 1–5.

[8] H. Wang, S. Sen, A. Elgohary, M. Farid, M. Youssef, and R. R. Choudhury, "No need to war-drive: unsupervised indoor localization," in *MobiSys*, 2012, pp. 197–210.

[9] M. Alzantot and M. Youssef, "Uptime: Ubiquitous pedestrian tracking using mobile phones," in *WCNC*, 2012, pp. 3204–3209.

[10] R. Want, A. Hopper, V. Falcao, and J. Gibbons, "The Active Badge Location System," in *ACM Transactions on Information Systems 10*, 1992, pp. 91–102.

[11] M. Youssef, M. Mah, and A. Agrawala, "Challenges: Device-Free Passive Localization for Wireless Environments," in *MobiCom '07: Proceedings of the 13th annual ACM international conference on Mobile computing and networking*. New York, NY, USA, 2007, pp. 222–229.

[12] Y. Yang and A. E. Fathy, "See-through-wall imaging using ultra-wideband short-pulse radar system," in *IEEE Antennas Propag. Soc. Int. Symp*, 2005.

[13] A. Lin and H. Ling, "Doppler and direction-of-arrival (DDOA) radar for multiple-mover sensing," *IEEE Trans. Aerosp. Electron. Syst.*, vol. 43, no. 4, pp. 1496–1509, 2007.

[14] A. M. Haimovich, R. S. Blum, and L. J. Cimini., "MIMO Radar with Widely Separated Antennas," *IEEE Signal Processing Magazine*, pp. 116–129, 2008.

[15] T. B. Moeslund, A. Hilton, and V. Krger, "A survey of advances in vision-based human motion capture and analysis," *Computer Vision and Image Understanding*, vol. 104, no. 2-3, pp. 90–126, 2006.

[16] J. Krumm, S. Harris, B. Meyers, B. Brumitt, M. Hale, and S. Shafer, "Multi-Camera Multi-Person Tracking for Easyliving," in *Third IEEE International Workshop on Visual Surveillance*, 2000.

[17] J. Wilson and N. Patwari, "Radio Tomographic Imaging with Wireless Networks," in *tech. rep.* University of Utah, 2008.

[18] M. Moussa and M. Youssef, "Smart Devices for Smart Environments: Device-free Passive Detection in Real Environments," in *IEEE PerCom Workshops*, 2009.

[19] A. E. Kosba, A. Saeed, and M. Youssef, "RASID: A Robust WLAN Device-free Passive Motion Detection System," in *PerCom*, 2012, pp. 180–189.

[20] M. Seifeldin and M. Youssef, "A Deterministic Large-scale Device-free Passive Localization System for Wireless Environments," in *PETRA '10: Proceedings of the 3rd International Conference on Pervasive Technologies Related to Assistive Environments*, 2010, pp. 1–8.

[21] I. Sabek and M. Youssef, "Multi-entity Device-Free WLAN Localization," in *IEEE Global Communications Conference, GlobeCom*, 2010.

[22] ——, "Spot: An Accurate and Efficient Multi-entity Device-Free Wlan Localization System," *CoRR*, vol. abs/1207.4265, 2012.

[23] N. Kassem, A. E. Kosba, and M. Youssef, "ReVISE: An RF-based vehicle detection and speed estimation," in *VTC Spring*, 2012.

[24] A. Lotfy and M. Youssef, "RF-based traffic detection and identification," in *VTC Fall*, 2012.

[25] A. Eleryan, M. Elsabagh, and M. Youssef, "Synthetic generation of radio maps for device-free passive localization," in *GLOBECOM*, 2011, pp. 1–5.

[26] K. El-Kafrawy, M. Youssef, and A. El-Keyi, "Impact of the human motion on the variance of the received signal strength of wireless links," in *PIMRC*, 2011, pp. 1208–1212.

[27] M. Seifeldin, A. El-keyi, and M. Youssef, "Kalman filter-based tracking of a device-free passive entity in wireless environments," in *Proceedings of the 6th ACM international workshop on Wireless network testbeds, experimental evaluation and characterization*. ACM, 2011, pp. 43–50.

[28] A. E. Kosba, A. Abdelkader, and M. Youssef, "Analysis of a device-free passive tracking system in typical wireless environments," in *The 3rd International Conference on New Technologies, Mobility and Security, NTMS*, 2009, pp. 1–5.

[29] D. Halperin, W. Hu, A. Sheth, and D. Wetherall, "Tool Release: Gathering 802.11n Traces with Channel State Information," *ACM SIGCOMM CCR*, vol. 41, no. 1, p. 53, Jan. 2011.

[30] D. Tse and P. Viswanath, *Fundamentals of wireless communication*. New York, NY, USA: Cambridge University Press, 2005.

[31] M. Seifeldin, A. Saeed, A. E. Kosba, A. El-Keyi, and M. Youssef, "Nuzzer: A large-scale device-free passive localization system for wireless environments," *IEEE Transactions on Mobile Computing*, 2012.